Dehydration of Xylose into Furfural in the Presence of Crystalline Microporous Silicoaluminophosphates

6 AUTHORS, INCLUDING:

Sérgio Lima
Imperial College London
43 PUBLICATIONS **1,073** CITATIONS

SEE PROFILE

Maria Antunes
University of Aveiro
23 PUBLICATIONS **504** CITATIONS

SEE PROFILE

Maria Filipa Ribeiro
Technical University of Lisbon
135 PUBLICATIONS **1,575** CITATIONS

SEE PROFILE

Anabela Valente
University of Aveiro
180 PUBLICATIONS **4,066** CITATIONS

SEE PROFILE

Dehydration of Xylose into Furfural in the Presence of Crystalline Microporous Silicoaluminophosphates

**Sérgio Lima · Auguste Fernandes ·
Margarida M. Antunes · Martyn Pillinger ·
Filipa Ribeiro · Anabela A. Valente**

Abstract Microporous silicoaluminophosphates SAPO-5, SAPO-11 and SAPO-40 have been tested as solid acid catalysts in the dehydration of xylose into furfural (FUR) under biphasic aqueous-organic conditions, at 170 °C. For all materials, no decrease in catalytic activity is observed after three consecutive recycling runs. Furfural yields at 4 h using SAPO-11 (34–38%) are comparable with that for HMOR zeolite with Si/Al ∼ 6 (34%), under similar reaction conditions, while H_2SO_4 (0.03 M) gives 2% FUR. Complete xylose conversion is reached within 16–24 h, with furfural yields of up to 65%. Brønsted and Lewis acidity of the silicoaluminophosphates was determined through FTIR analysis of adsorbed pyridine, and tentatively correlated with the catalytic performances.

Keywords Xylose · Furfural · Dehydration · Silicoaluminophosphate · Microporous · Solid acid

1 Introduction

The processing of plant biomass-derived carbohydrates into added-value products is at the core of the biorefinery concept. In particular, the acid-catalysed hydrolysis and dehydration of saccharides, which constitute the bulk of carbohydrates, into furfural (FUR) and 5-hydroxymethyl-2-furfuraldehyde (HMF) are important processes, since these are platform chemicals for generating a variety of nonpetroleum derived products [1–3]. Sulfuric acid is commonly used in industry as the catalyst for FUR production, presenting several disadvantages [3]. Recent research has focussed on the replacement of the "toxic liquid" acid catalysts by stable, recyclable, non-toxic solid acids based on inorganic oxides [4–10]. The development of water-tolerant heterogeneous catalysts is crucial since water is the preferred solvent for the reactions mentioned above, and this can level off the surface acidity of solid acids [10].

Two of the most commonly studied types of microporous solid acids are zeolites (aluminosilicates) and silico-aluminophosphates (SAPOs). In SAPOs, the introduction of Si atoms in $AlPO_4$ frameworks leads to the appearance of negative charges that are balanced by protons attached to Si–O–Al bridges, thereby originating Brønsted acidity. The Si substitution can be for phosphorus (SM2 mechanism) or an aluminium-phosphorus pair (SM3 mechanism) [11, 12]. The amount of silicon incorporated via SM2 is always limited, and above certain Si contents both mechanisms occur. The SM3 mechanism generates isolated pairs of Si atoms with Si in Si(1Si3Al) and Si(1Si3P) configurations [11] leading to extended Si islands and various acid site environments with variable number and strength. A higher number of acid sites are generated through the first mechanism (SM2), while the second yields less but stronger acid sites [12]. For these reasons, the acidity of SAPOs is sometimes considered to be more tuneable than that of zeolites [11, 12]. In a study of zeolites with different framework types (BEA, FAU, MFI, MOR) for the dehydration of monosaccharides, favorable shape selective

S. Lima · M. M. Antunes · M. Pillinger · A. A. Valente (✉)
Department of Chemistry, CICECO, University of Aveiro,
Campus de Santiago, 3810-193 Aveiro, Portugal
e-mail: atav@ua.pt

M. Pillinger
e-mail: mpillinger@ua.pt

A. Fernandes · F. Ribeiro
Institute of Biotechnology and Bioengineering,
Instituto Superior Técnico, Av. Rovisco Pais, 1049-001 Lisbon,
Portugal

effects were reported for MOR, which possesses sufficiently large channels (6.5 × 7.0 Å) running in one direction [5, 13, 14]. Motivated by these findings, we set out to screen the catalytic performance of SAPOs containing medium or large pore channels, namely SAPO-5, SAPO-11 and SAPO-40, in the dehydration of xylose to FUR.

2 Experimental

2.1 Catalyst Preparation and Characterisation

The SAPO-5 and SAPO-40 samples were prepared as described in the literature [15, 16]. Two SAPO-11 samples with different morphologies and crystal size were synthesized following conventional [dipropylamine template (DPA)] and modified (DPA and methylamine (MA) co-templates) synthesis strategies [17]; the compositions (molar ratio) of the initial gels were $Al_2O_3:P_2O_5:0.66$-$SiO_2:1.5DPA:40H_2O$ and $Al_2O_3:P_2O_5:0.6SiO_2:DPA:0.3$-$MA:50H_2O$, respectively. Both preparations were subjected to crystallization under autogeneous pressure at 200 °C during 24 h.

Powder X-ray diffraction (XRD) data were collected for all samples at room temperature on a Philips X'Pert MPD diffractometer, equipped with an X'Celerator detector, a graphite monochromator (Cu-K$_\alpha$ X-radiation, λ = 1.54060 Å) and a flat-plate sample holder, in a Bragg–Brentano para-focusing optics configuration (40 kV, 50 mA). Samples were step-scanned in 0.04° 2θ steps with a counting time of 6 s per step. SEM was carried out on a Hitachi SU-70 UHR Schottky instrument. ICP-AES was performed on a Horiba Jobin Yvon Activa-M spectrometer. The BET specific surface areas (S_{BET}) were estimated from N_2 adsorption isotherms measured at −196 °C using a Micromeritics ASAP 2010 instrument. Samples were outgassed at 350 °C under vacuum. The external surface areas (S_{ext}) and micropore volumes (V_{micro}) were obtained using the t-plot method. The acid properties were measured using a Nexus-Thermo Nicolet apparatus (64 scans and resolution of 4 cm^{-1}) equipped with a specially designed cell, using self-supported discs (5–10 mg sample cm^{-2}) and pyridine as the basic probe. After in situ outgassing at 450 °C for 3 h (10^{-6} mbar), pyridine (99.99%) was contacted with the sample at 150 °C for 10 min and then evacuated at 150 and 350 °C (30 min) under vacuum (10^{-6} mbar). The IR bands at ca. 1,540 and 1,455 cm^{-1} are related to pyridine adsorbed on Brønsted (B) and Lewis (L) acid sites, respectively [18]. Thermogravimetric analysis (TGA) and differential scanning calorimetry (DSC) were carried out under air using Shimadzu TGA-50 and DSC-50 systems.

2.2 Catalysis Tests

The batch catalytic experiments were performed under nitrogen as described elsewhere [8, 19, 20]. Typically, D-xylose (30 mg), powdered catalyst (20 mg) and a solvent mixture comprising H_2O (0.3 mL) and toluene (0.7 mL) were poured into the reactor. The reaction mixtures were heated at 170 °C with a thermostated oil bath and stirred at 600 rpm (optimized to avoid external mass transfer limitations). Under these conditions, the reaction of xylose takes place in the aqueous phase (where it dissolves completely) and the product furfural transfers to the organic phase. Without a catalyst, the aqueous phase reaction of xylose gives 5% furfural yield after 6 h at 170 °C; throughout the discussion the results have not been corrected for this non-catalytic contribution. Furfural selectivity (%) is calculated using the formula: (number of moles of furfural formed)/(number of moles of xylose consumed) × 100.

The products present in the aqueous phase were analyzed using a Knauer K-1001 HPLC pump and a PL Hi-Plex H 300 × 7.7 (i.d.) mm ion exchange column (Polymer Laboratories Ltd, UK), coupled to a Knauer 2300 differential refractive index detector (for xylose) and a Knauer 2600 UV detector (280 nm, for furfural). The mobile phase was 0.01 M H_2SO_4. The analysis conditions comprised a flow rate of 0.6 mL min^{-1} and a column temperature of 65 °C. The furfural present in the organic phase was quantified using a Gilson 306 HPLC pump and a Spherisorb ODS S10 C18 column, coupled to a Gilson 118 UV/Vis detector (280 nm). The mobile phase (flow rate 0.5 mL min^{-1}) consisted of 30% v/v methanol in an aqueous solution mixed with 10% methanol. Authentic samples of D-xylose and furfural were used as standards, and calibration curves were used for quantification.

3 Results and Discussion

3.1 Characterisation

Figure 1 shows the powder XRD patterns for the as-synthesized and calcined SAPO-5, SAPO-11 and SAPO-40 samples. The XRD patterns of the as-synthesized materials are identical to those reported in literature [21]. Table 1 collects the texture properties and chemical formulae of the four samples. Both SAPO-11 samples exhibit pseudo-spherical aggregates: SAPO-11b, prepared using the MA-based procedure, possesses aggregates with sizes comprised between 20 and 30 μm, while SAPO-11a prepared using the MA-free procedure possesses smaller aggregates in the range 1–5 μm (Fig. 2). These results are consistent with those reported for SAPO-11 materials

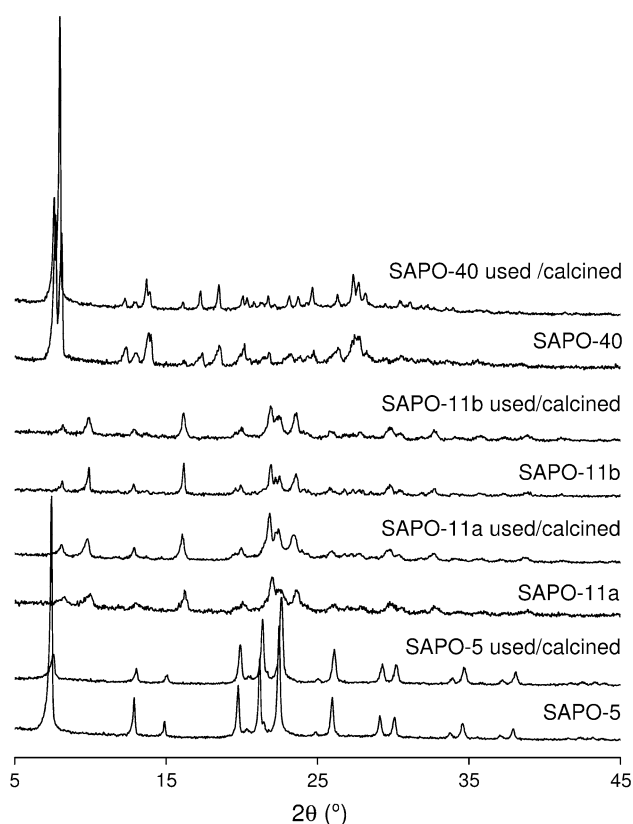**Fig. 1** Powder XRD patterns of the fresh and used SAPO materials

Table 1 Structural and texture properties of the SAPOs

Sample	Formula	S_{BET} (m^2/g)	S_{ext} (m^2/g)	V_{micro} (cm^3/g)
SAPO-5	$Al_{0.49}P_{0.47}Si_{0.04}O_2$	312	25	0.13
SAPO-11a	$Al_{0.45}P_{0.42}Si_{0.13}O_2$	274	43	0.10
SAPO-11b	$Al_{0.49}P_{0.41}Si_{0.10}O_2$	241	43	0.08
SAPO-40	$Al_{0.46}P_{0.47}Si_{0.07}O_2$	670	60	0.27

3.2 Catalysis

The reaction of xylose at 170 °C in the presence of the SAPOs gives 58–65% FUR selectivity at 100% conversion, reached within 16–24 h (Fig. 3b). A similar FUR yield of 63% was reported for the aqueous-phase reaction of xylose (with an initial concentration of 0.05 M) in the presence of 0.03 M H_2SO_4 at 250 °C [26]. Under similar reaction conditions to those used in the present study, H_2SO_4 (0.03 M) gives 2% FUR selectivity at 98% conversion (4 h reaction). For the SAPOs, factors which may favour FUR production are shape selectivity, acid properties (e.g. *L/B* ratio, as discussed below), and competitive adsorption effects. The reaction in the presence of the SAPO-11 samples gives FUR yields at 4 h of 34–38%, which are comparable with that obtained for HMOR zeolite with Si/ Al ~ 6 (34% FUR yield at 4 h), under similar reaction conditions [9].

The materials used in this work have different crystalline structures: SAPO-5 (AFI structure) and SAPO-11 (AEL structure) consist of 1D channel systems with pore openings of 7.3 × 7.3 Å and 6.4 × 4.4 Å, respectively, while SAPO-40 with the AFR structure consists of a 2D channel system with pore openings of 6.7 × 6.9 Å and 3.7 × 3.7 Å. The molecular diameters (along the longest axis) of xylose and furfural are 6.8 and 5.7 Å, respectively [27]. Considering that the "catalytic pore sizes" of zeolites are often found to exceed the crystallographic ones (by as much as 2 Å in the case of H-MOR, for example) [28], the xylose molecules may be able to diffuse into the channels of all three framework types, under the reaction conditions used for catalysis. Indeed, according to the literature, the 8.6 Å glucose molecule is able to diffuse into the water-filled 7.4 Å Y-zeolite pore [29]. In the liquid phase the solute diffuses as a solute–solvent assemblage and catalyst-solvent interactions may reduce the effective diffusivity of xylose within the liquid-filled pores of the SAPO materials. On the other hand, diffusivity depends on factors such as reaction temperature and viscosity of the fluid, and diffusion may be facilitated at higher temperatures. Smaller crystallite/particle sizes may enhance the overall reaction rate by increasing the number of accessible acid sites and decreasing the intracrystalline diffusion path lengths.

prepared using the same procedures [17]. Commonly observed morphologies of hexagonal prism-shaped crystals of size 3–10 μm are observed for SAPO-5 [22] and flat tabular crystals of length 2–10 μm for SAPO-40 [23].

The Brønsted (*B*) and Lewis (*L*) acid properties of the silicoaluminophosphates were quantified by adsorption of pyridine followed by FTIR (Table 2). Pyridine was chosen as the basic probe since its critical dimension of ca. 6.5 Å [24] is comparable with the size of the xylose molecule. All the samples show both *L* and *B* sites interacting with pyridine after outgassing at 150 °C. The total acidity is around 120 μmol g^{-1} for the SAPO-5 and SAPO-11 samples, and 459 μmol g^{-1} for SAPO-40. However, whereas [*B*] increases greatly on going from SAPO-5 and SAPO-11 to SAPO-40, the [*L*] decreases. Although the *L* sites are probably due to defective framework and/or extra-framework Al species, we cannot exclude the possibility that *L* sites may arise from changes in the coordination of framework Al atoms upon interaction with the basic probe [25]. At 350 °C pyridine desorbed more easily from the *B* sites than from the *L* sites. Thus, the ratio moderate + strong to total Brønsted sites ([*B*]$_{350}$/[*B*]$_{150}$) is in the range of 0.07–0.19 for all four materials, indicating that most of the sites are of a rather weak nature, while the Lewis ratio ([*L*]$_{350}$/[*L*]$_{150}$) is nearly 0.5 for the SAPO-5 and SAPO-11 samples, and unity for SAPO-40.
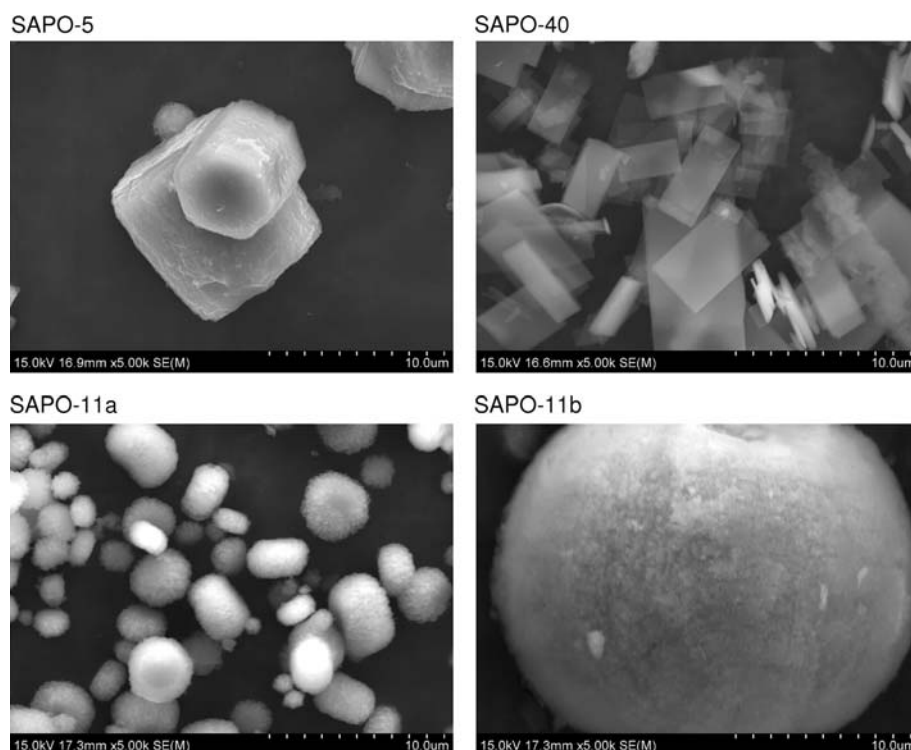
Fig. 2 SEM images of the SAPO materials

Table 2 Acid properties of the SAPOs

Sample	$[L] + [B]$ (μmol g^{-1})[a]	$[B]$ (μmol g^{-1})[a]	$[L]/[B]$[a]	$[L]_{350}/[L]_{150}$	$[B]_{350}/[B]_{150}$
SAPO-5	124	78	0.58	0.48	0.07
SAPO-11a	119	52	1.30	0.45	0.12
SAPO-11b	111	75	0.48	0.46	0.19
SAPO-40	459	452	0.01	1	0.12

[a] Measured at 150 °C

To probe the existence of such effects, the catalytic activities of two SAPO-11 materials possessing different particle sizes have been compared. The conversion versus time curves for SAPO-11a (1–5 μm) and SAPO-11b (20–20 μm) are roughly coincident (Fig. 3a). SEM images for the recovered SAPO-11a and SAPO-11b solids did not show significant morphological changes (not shown here). These results suggest that the overall reaction is not strongly diffusion limited. It is noticeable that (1) the similar reaction rate correlates with the similar total acidity [8], and (2) for conversions up to about 75%, the FUR selectivities are somewhat higher for SAPO-11b than for SAPO-11a (Fig. 3b). The differences in FUR selectivities may be partly due to differences in the *L/B* ratio (Table 2). While there are no major differences in terms of acid strengths between the SAPO-11 samples, the number of *L* sites detected for SAPO-11a is nearly double that found for SAPO-11b, and the amount of *B* sites detected for SAPO-11b is ca. 1.5 times that found for SAPO-11a. In the reaction temperature range of 160–180 °C, the reaction rates (based on conversions at 2 and 4 h) increase with

temperature and the two SAPO-11 materials give comparable conversions (Table 3). Similar to that observed for 170 °C, when the reaction is carried out at 160 or 180 °C, FUR selectivities at similar xylose conversions are somewhat higher for SAPO-11b than for SAPO-11a.

The SAPO-11b and SAPO-5 samples exhibit comparable texture and acid properties, but the reaction is slower for SAPO-5 (Fig. 3a). When calculated on the basis of surface area, the reaction rates (μmol h^{-1} m$_{cat}^{-2}$) at 30 min and 4 h reaction follow the order (rates at 30 min; 4 h): SAPO-5 (0.13; 0.06) < SAPO-11a (0.41; 0.13) $\cong$ SAPO-11b (0.46; 0.14). As could be expected (the specific surface areas are comparable), similar trend is observed for rates calculated at the same time points on the basis of the catalyst mass (μmol h^{-1} g$_{cat}^{-1}$): SAPO-5 (41; 17) < SAPO-11a (111; 37) $\cong$ SAPO-11b (111; 35). On the other hand, even though SAPO-40 possesses the highest total acidity and the highest number of moderate + strong acid sites (those retaining pyridine at 350 °C), as well as the highest S_{BET}, S_{ext} and V_{micro}, the reaction rate (on the basis of the mass of catalyst) is comparable with that observed for SAPO-5.
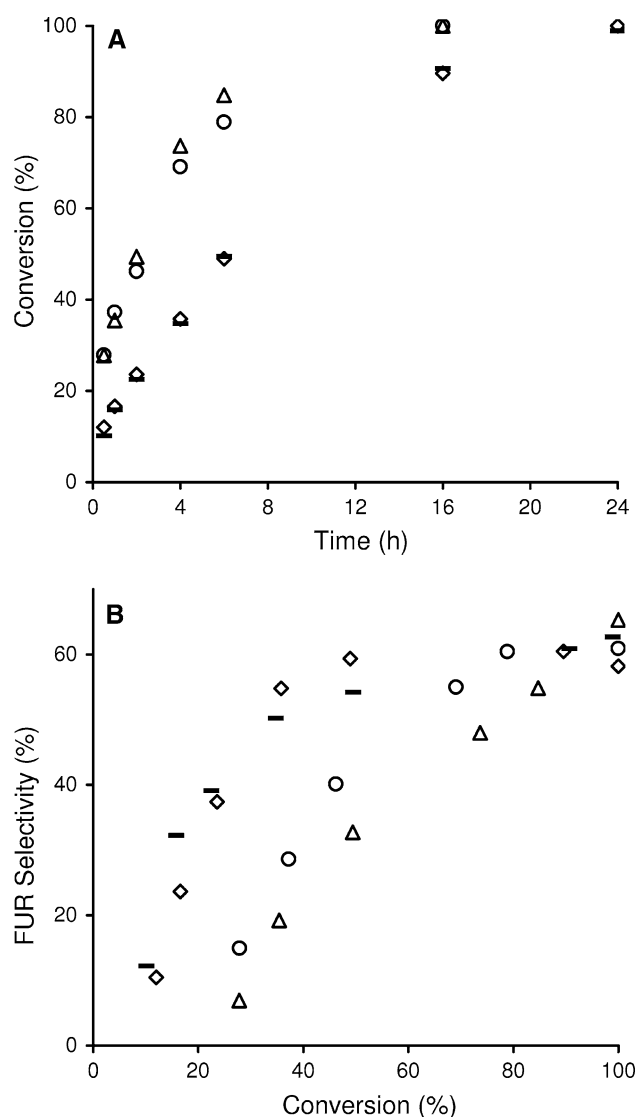
Fig. 3 Kinetic profiles of the xylose reaction (**a**) and dependence of furfural selectivity on conversion (**b**), in the presence of SAPO-5 (*filled rectangle*), SAPO-11a (*open triangle*), SAPO-11b (*open circle*) and SAPO-40 (*open diamond*), at 170 °C

Table 3 Conversion of xylose into FUR in the presence of SAPO-11 materials, at 160–180 °C

|	Temperature (°C)	Conversion at 2 h/4 h (%)	FUR selectivity at 2 h/4 h (%)
SAPO-11a	160	29/46	31/50
	170	49/74	33/48
	180	76/99	26/42
SAPO-11b	160	26/49	47/58
	170	46/69	40/55
	180	73/96	37/53

Given the complexity of the catalytic systems it is difficult to correlate the different reaction rates with the strengths and densities of the acid sites for the different framework structures, and it is thus preferable to restrict the correlations to a specific structure type, as discussed above for SAPO-11.

The observed increase in FUR selectivity with time for all catalysts has been noted with other solid acid catalysts [8, 9, 19] and is probably due to the complex reaction mechanism involving a series of elementary steps for producing FUR, where the disappearance of xylose is possibly not rate limiting [3, 26]. In the net conversion of xylose to FUR, three water molecules are formed per molecule of FUR (Scheme 1). On the other hand, the influence of competitive adsorption effects and changes in the surface properties of the catalysts during the reaction cannot be ruled out. The FUR selectivity is always less than 100% and the originally white powders turn light brown during the reactions. No by-products were detected by gas (GC-MS of the toluene phase) or liquid (differential refractive index detector and UV diode-array detection mode for the aqueous phase) chromatography, possibly because they are insoluble, "non-volatile" organic compounds, which are responsible for the brown colour. For the SAPO-11 materials the amount of this insoluble matter formed after 16 h reaction was estimated by removing all solids from the reaction medium by filtration, drying, weighing and subtracting the initial amount of catalyst. The "excess" weight corresponded to ca. 20 wt% of the initial amount of xylose. Using this result, the wt% balance of FUR (based on the initial amount of xylose) nearly closes: (wt% solid by-products) + (wt% yield of FUR) = 59–61 wt% FUR, compared with the theoretical yield of 64 wt%.

Differential scanning calorimetry analyses (not shown) of the fresh and used (washed with methanol and a 50% v/v mixture of water/ethanol, and dried at 65 °C) solids showed endothermic bands below 200 °C assigned to physisorbed water and volatiles. Above 200 °C, all used catalysts exhibited exothermic bands not presented by the original catalysts. TGA analyses of used catalysts in the temperature range of 200–550 °C indicated weight losses of 2.8–5.1%, confirming the presence of organic by-products in the washed and dried solids. The specific surface areas of the used/washed/dried SAPO-11 materials decreased significantly by a factor of ca. 12. When the washed/dried SAPO-11a was used in a second run of the xylose reaction, the FUR yield at 4 h decreased ca. 10%. Hence, the efficient regeneration of the SAPOs requires removal of the organic matter, which may be accomplished by thermal treatment under air to promote the total oxidation of the carbonaceous matter.

The stability of the catalysts was further investigated by applying a thermal treatment (1° min^{-1} until 450 °C, 3 h, under air) after washing/drying the materials and prior to their reuse (three consecutive 4 h batch runs were
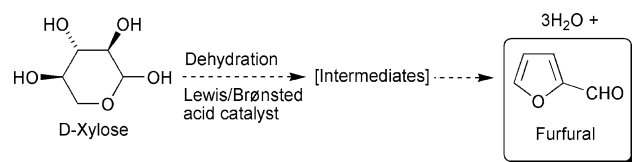
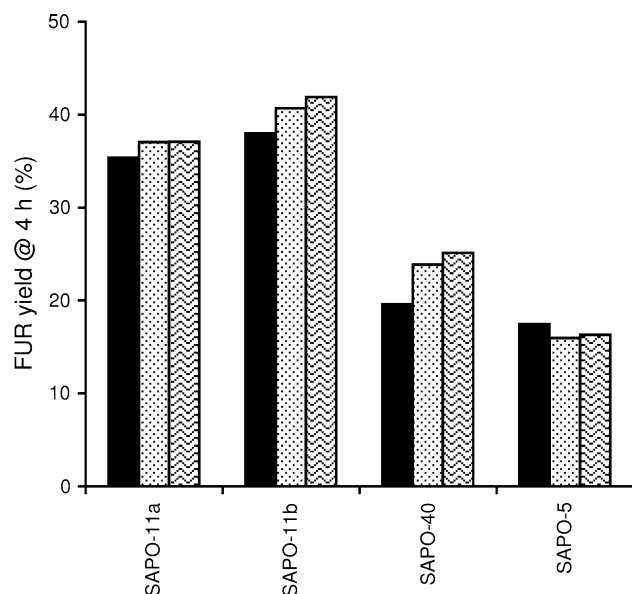Scheme 1 Simplified reaction mechanism of the xylose reaction to give FUR

Fig. 4 Furfural yields in recycling runs (run1—*solid black*, run2—*dots*, run3—*waves*) in the presence of the SAPOs (4 h runs, 170 °C)

performed for each sample). No significant decrease in FUR yield is observed for any of the samples in the three consecutive runs (Fig. 4). The powder XRD patterns of the fresh and recovered catalysts are quite similar indicating that the respective crystalline structures are preserved (Fig. 1). ICP-AES analyses for the recovered SAPO-5, SAPO-11b and SAPO-40 samples showed no decrease in Si, P or Al contents (experimental error: ca. 10%). Hence, the SAPO solid acids seem to be fairly stable under the reaction conditions used.

4 Conclusion

In this work we have demonstrated that medium pore and large pore SAPO molecular sieves can be used as recyclable solid acids for the dehydration of xylose into furfural under aqueous-organic biphasic conditions. The similar reaction rate for the SAPO-11 materials correlated with the similar total acidity, and the differences in FUR selectivities may be partly due to differences in the *L/B* ratio. Although the SAPO-11 system seems to be the most promising in this study (giving FUR yields at 4 h of 34–

38%, comparable with HMOR zeolite with Si/Al $\sim$ 6), the latter is limited within the versatile SAPO systems and it is possible that others exhibit superior catalytic performances. On the other hand, for a specific SAPO system the catalytic performance may be fine-tuned, based on detailed/systematic investigations of the effects of the preparation method, crystallinity, morphology, silicon content and acidity on the catalytic performances: these studies may also provide insights into the factors that influence the target versus undesired reaction pathways.

When compared with other solid acids investigated by our group (namely Nb-MCM-41 [30], cesium salts of 12-tungstophosphoric acid and mesoporous silica-supported 12-tungstophosphoric acid [31, 32], bulk and mesostructured sulfated zirconia [33]), the investigated SAPO materials present superior stability towards leaching phenomena (i.e., are more water-tolerant) when tested in the same reaction under comparable reaction conditions. Water-tolerant solid acids derived from the layered zeolite Nu-6(1) [9] and from exfoliated Ti and/or Nb layered oxides [8] exhibit higher catalytic activity in comparison to the SAPO materials. However, the maximum FUR yields achievable by these families of materials are somewhat comparable and, considering the catalyst preparation process, the SAPO materials are more convenient since they do not require the extensive post-synthesis modifications necessary to increase the specific surface areas (and to improve the accessibility of the active sites) of the above mentioned layered materials.

References

1. Leshkov YR, Chheda JN, Dumesic JA (2006) Science 312:933
2. Chheda JN, Leshkov YR, Dumesic JA (2007) Green Chem 9:342
3. Zeitsch KJ (2000) The chemistry and technology of furfural and its many by-products. In: Sugar Series, 1st edn, vol. 13. Elsevier, The Netherlands
4. Lourvanij K, Rorrer G (1993) Ind Eng Chem Res 32:11
5. Moreau C, Durand R, Pourcheron C, Razigade S (1994) Ind Crop Prod 3:85
6. Moreau C (2002) Agro-food-industry hi-tech 17
7. Carlini C, Patrono P, Galletti AMR, Sbrana G (2004) Appl Catal A: Gen 275:111
8. Dias AS, Lima S, Carriazo D, Rives V, Pillinger M, Valente AA (2006) J Catal 244:230
9. Lima S, Pillinger M, Valente AA (2008) Catal Commun 9:2144
10. Rinaldi R, Schüth F (2009) Energy Environ Sci 2:610
11. Mertens M, Martens JA, Grobet PJ, Jacobs PA (1990) In: Barthomeuf D, Derouane EG, Hölderich W (eds) Guidelines for

mastering the properties of molecular sieves. Plenum Press, New York, p 1

12. Pastore HO, Coluccia S, Marchese L (2005) Annu Rev Mater Res 35:351
13. Moreau C, Durand R, Razigade S, Duhamet J, Faugeras P, Rivalier P, Ros P, Avignon G (1996) Appl Catal A: Gen 145:211
14. Moreau C, Durand R, Peyrin D, Duhamet J, Rivalier P (1998) Ind Crops Prod 7:95
15. Weyda H, Lechert H (1990) Zeolites 10:251
16. Lourenço JP, Ribeiro MF, Ribeiro FR, Rocha J, Gabelica Z, Derouane EG (1995) Microporous Mater 4:445
17. Fernandes A, Ribeiro MF, Lourenço JP, Gabelica Z (2008) Stud Surf Sci Catal 174:281
18. Campelo JM, Lafont F, Marinas JM (1995) J Chem Soc Faraday Trans 91:1551
19. Dias AS, Pillinger M, Valente AA (2005) J Catal 229:414
20. Dias AS, Pillinger M, Valente AA (2005) Appl Catal A: Gen 285:126
21. Lok BM, Messina CA, Patton RL, Gajek RT, Cannan TR, Flaningen E (1984) US Patent 4,440,871
22. Sinha AK, Sainkar S, Sivasanker S (1999) Microporous Mesoporous Mater 31:321
23. Renzo FD, Dumont N, Trens P, Gabelica Z (2003) J Cryst Growth 259:160
24. Webster CE, Drago RS, Zerner MC (1998) J Am Chem Soc 120:5509
25. Derewinski M, Briend M, Peltre MJ, Man PP, Barthomeuf D (1993) J Phys Chem 97:13730
26. Antal MJ, Leesomboon T, Mok WS, Richards GN (1991) Carbohydr Res 217:71
27. O'Neill R, Ahmad MN, Vanoye L, Aiouache F (2009) Ind Eng Chem Res 48:4300
28. Webster CE, Drago RS, Zerner MC (1999) J Phys Chem B 103:1242, and references cited therein
29. Netrabukkana R, Lourvanij K, Rorrer GL (1996) Ind Eng Chem Res 35:458
30. Dias AS, Lima S, Brandão P, Pillinger M, Rocha J, Valente AA (2006) Catal Lett 108:179
31. Dias AS, Pillinger M, Valente AA (2006) Microporous Mesoporous Mater 94:214
32. Dias AS, Lima S, Pillinger M, Valente AA (2006) Carbohydr Res 341:2946
33. Dias AS, Lima S, Pillinger M, Valente AA (2007) Catal Lett 114:151